

The Nippon/Norway Svalbard Meteor Radar : First results of small-scale structure observations

CM Hall¹ , BO Husøy¹ , T Aso² and M Tsutsumi²

¹ Tromsø Geophysical Observatory , Tromsø , Norway

² National Institute of Polar Research , Tokyo 173 , Japan

Received October 24 , 2001

Abstract The Nippon/Norway Svalbard Meteor Radar (NSMR) , has been in operation since March 2001. While primarily thought of as an instrument for examining mean wind , tidal and gravity wave neutral atmosphere dynamics in the upper mesosphere region , it is also possible to investigate spatial and temporal structure of temperature and windshear. Here , the radar itself is described followed by a presentation of these derived parameters.

Key words middle atmosphere dynamics , meteor radar , polar region.

1 Introduction

At latitudes around 80°N and in the mesosphere / lower thermosphere (MLT) , there have been few measurements of neutral dynamics. A requirement was seen for long term continual monitoring and a VHF meteor radar was identified as being a most suitable instrument. Radars like the EISCAT Svalbard radar (Wannberg *et al.* 1997) , the SOUSY Svalbard Radar (Røttger 2000) take measurements sporadically and furthermore experience problems obtaining echoes from the mesosphere during night time (e.g. Hall and Aso 1999) due to lack of ionisation. On the other hand , a meteor radar makes use of ionisation trails from meteors and is neither reliant on particle precipitation nor on insolation. An introduction to such systems may be found in Tsutsumi *et al.* (1999).

The site chosen for NSMR was in Adventdalen at 78.2°N , 16.0°E , collocated with the SSR (Fig.1). The system , supplied by ATRAD (<http://www.atrad.com.au>) consists of one transmitter antenna with a half power half width of 45° thus illuminating a wide area of the sky in order to “ catch ” as many meteors as possible. The receiver array consists of a “ Jones *et al.* cross ” : one centre antenna , two adjacent orthogonal arms with antennae 2.5 wavelengths from the centre , and two adjacent orthogonal arms with antennae 2.0 wavelengths from the centre (Jones *et al.* 1998). This receiver array functions as an interferometer permitting angles of arrival of meteors and the resulting Doppler shifts of their trails to be determined. In addition , the decay times of the meteor echoes are indicative of the ambipolar diffusion coefficients of the ions forming the trails. The salient features of the radar are given in Table 1. and Fig.2 shows an aspect of the radar itself.

Table 1. Salient features of NSMR (current as of summer 2001)

Parameter	Value
Geographic coordinates	78.17°N , 16.00°E
Operating frequency	31.0 MHz
Pulse repetition frequency	500 Hz
Coherent integrations	4
Pulse length(range resolution)	6.7 μ s (2 km)
Peak power(10% duty cycle)	7.5 kW
Transmitter antenna	3-way (60°) crossed dipole
Receiver antennae	5 crossed (orthogonal) dipoles as interferometer
Antenna beamwidth	90° full width at half power
Antenna one way gain	33 dB



Fig.1. Location of NSMR(Nippon / Norwegian Svalbard Meteor Radar) , near Longyearbyen. The longitude at the centre of the map is 20°E.

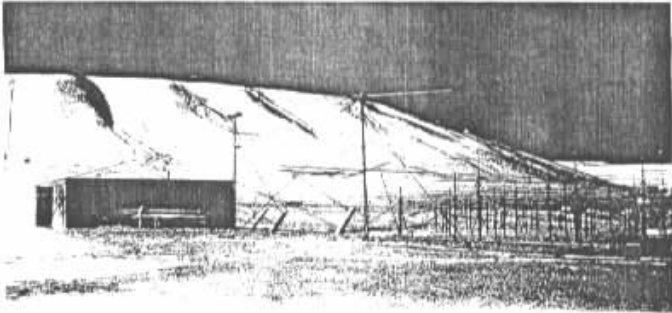


Fig.2. Night-time view , looking east , of part of the NSMR location. The NSMR transmitter antenna is in the centre foreground. The antenna field to the right is that of the SSR(SOUSSY Svalbard Radar). The nearest building(container) to the left houses both the SSR and NSMR transmitters and receivers , computer hardware and WAN connectivity. Buildings further back are for storage and office. Other antennae include GPS , aircraft proximity warning radar (for automatic shutdown of radars) and communication with the local air traffic control. One of Svalbard 's disused coalmines , " mine 6 " can be seen just right of centre on the mountainside in the background.

Fig.3 shows one day 's " meteors ". In the left-hand panel we show the positions of meteor echoes with respect to the radar location. Note that a single meteor may give rise to several e-

choes along its flight path. On Svalbard most meteors traverse the sky since the Earth's and the meteors' orbits are quasi coplanar and the latitude is high. In contrast, an equatorial station would see strong diurnal and directional preferences, and also a proportion of meteors arrive "head-on". We see, in the right-hand panel, that the preferred altitude is 90 km. Due to the relatively even distribution of echoes in time and space, we see that high latitude meteor radars are well suited to tidal observation, at least at 90 km.

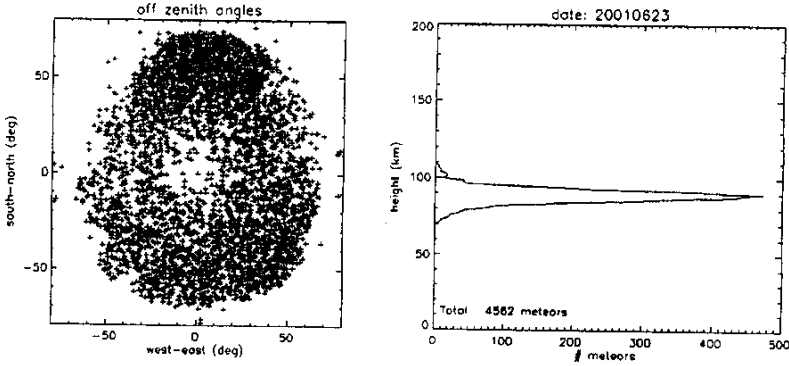


Fig.3. Distributions of echoes for a typical day. Left : Positions of meteor echoes relative to the radar. Each cross represents an echo, and it is not unusual for one meteor to give rise to 2 or 3 successive echoes, although one echo is more usual. Axes denote azimuth. Right : distribution of echoes with height. The total number of echoes in this case was 4562.

A fuller description of NSMR is given by Aso *et al.* (2001)*. Introductions to meteor radar theory may be found in, for example, Tsutsumi *et al.* (1994), Hocking and Thayaparan (1997), Hocking *et al.* (1997) and Hocking (1999), in which derivation of the various parameters discussed below are explained.

2 Diffusivity and temperature

As stated above, it is possible to determine the ambipolar diffusion coefficient of the ions responsible for the echo. This is quite simply done by measuring the characteristic fading time of the echo : e.g. the time for the amplitude to drop to half or $1/e$ of its initial value, or a similar metric. However, in practice this approach is obviously too simplistic (e.g. Jones 1995); rather than the resulting diffusion coefficient exhibiting a well-behaved exponential increase with altitude, there are tendencies towards constant values in the mid-mesosphere and decreasing values in the lower thermosphere. The following phenomena presumably affect the diffusion profile shape :

- (a) neutral air turbulence begins to affect the echo fading at the lowest altitudes.
- (b) electrodynamics affects the ion motion at the highest altitudes (Dyrud *et al.* 2001).

* Aso T, Tsutsumi M, Hall CM (2001) : First results of NSMR-Nippon/Norway Svalbard Meteor Radar-observations in Longyearbyen in early 2001. submitted to Annales Geophys.

(c) the ion species is open to debate : it may be a mixture of metal ions (i.e. ablation of the meteor) or nitrogen (i.e. the ambient gas is ionised by the meteor 's passage) , and this may vary with height .

Despite these problems , it is possible to see a seasonal dependence in the diffusivity as presented in Fig. 4. Again it should be stressed that the above problems pertain to these data and therefore little significance should be attached to the absolute values of ambipolar diffusion coefficient shown here. However it is interesting to note the transition from the winter to summer state , around the end of May .

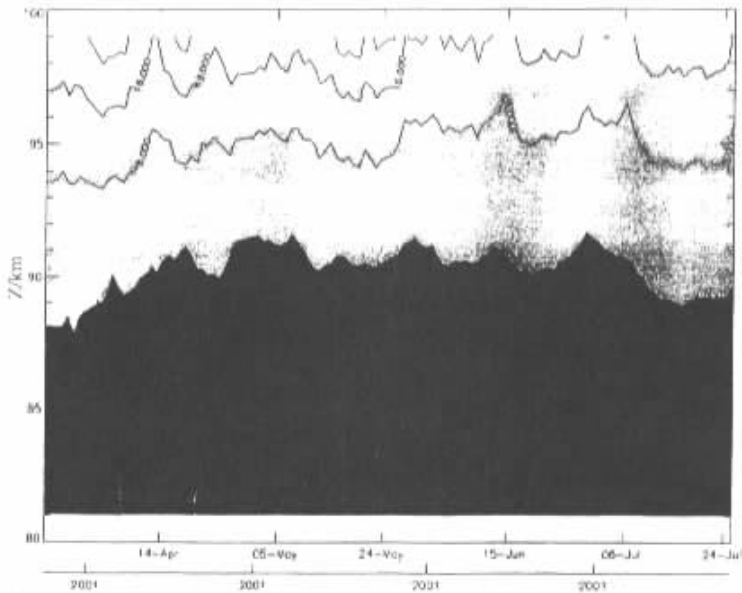


Fig.4. Ambipolar diffusion coefficient as a function of height and time. Units are in m^2s^{-1} . The absolute values are subject to the uncertainties described in the text. Note the spring to summer transition in the lower centre of the plot.

By employing a neutral density model such as MSISE90(Hedin 1991) it is possible to estimate temperatures from the ambipolar diffusivities (e.g. Hocking 1999). For reasons unclear , however , the resulting temperatures rarely agree with expectations (models and observations) and it is not uncommon to apply some correction factor to the resulting temperature profile (again , Hocking 1999). This correction does not appear to be universal and we have chosen to normalize to a typical MSISE90 spring temperature profile and allow the other profiles to “ float ” with respect to this normalization. Again , as for diffusivity , there are underlying assumptions and uncertainties , so rather than focus on the absolute values of the resulting temperature estimates , we rather concentrate on relative temporal and spatial variation : Fig.5 shows the development of mesospheric temperature through spring to summer 2001. Of considerable interest here is the evidence for a mesopause rather higher up than observed at , say , 70°N. This mesopause height , over 90 km , has been confirmed by lidar observations from the SSR site(R⁹ ttger , private communication).

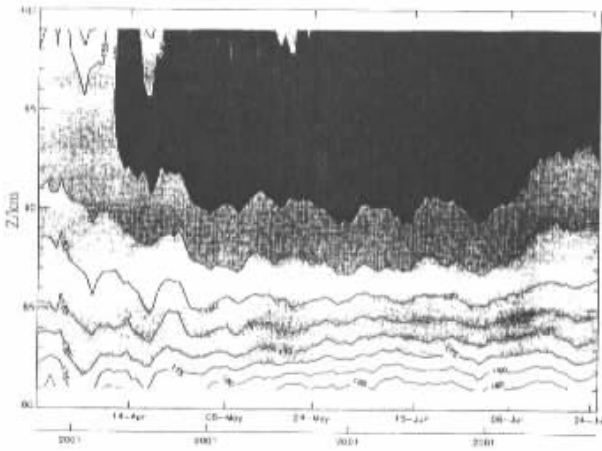


Fig. 5. Temperature estimates corresponding to the diffusivities in the previous figure. Again certain assumptions are implicit here and the absolute values (in K) are not to be relied upon. Note the emergence of the summer mesopause in the upper right portion of the plot.

3 Wind shear

In order to derive daily parameters from the meteor trail echoes, it has been suggested by W Hocking (private communication) that 600 echoes are required to provide statistical significance. We can see from Fig. 3 that this condition is fulfilled and moreover we obtain spatial and temporal distributions adequate to estimating winds every 30 min with a 1 km height resolution. By determining the vector difference between winds U , at adjacent altitudes z , it is therefore possible to deduce windshear as a function of height. Obtaining the Brunt-Väisälä frequency ω_B from the model temperatures provided by MSISE90 (rather than rely on the meteor radar temperature estimates, for reasons explained earlier) we are able to estimate the gradient Richardson number Ri :

$$Ri(z) = \omega_B^2(z) / (dU/dz)^2$$

The gradient Richardson number is commonly used as a determination of the dynamic stability of the atmosphere. Indeed, if the Brunt-Väisälä frequency is imaginary, indicating a convective instability, we also see that when $Ri < 0$ the atmosphere is convectively unstable. The condition $0 < Ri < 0.25$ is generally accepted as an indication of dynamic instability; if $Ri < 0.4$, any existing turbulence could be expected to be enhanced, or at least maintained (Roper and Brosnahan 1997). We have determined daily averages of Ri since the start of radar operations. In Fig. 6, we present these estimates from three different heights (88, 90 and 92 km) both as daily means themselves and as daily means minus the 1-sigma variability (standard deviation). Since turbulence occurs on timescales of less than one day it is reasonable to assume that during some of each day Ri will achieve values shown by the mean minus 1-sigma value. Since we have obtained ω_B from a model that indicates a convectively stable mesosphere, negative values of Ri are never incurred. However, we see that on many occasions dynamic instability is indicated. Furthermore these instabilities are features of the atmosphere prior to the onset of the summer state (c.f. temperature results in Fig. 4). Note also that convective instabilities may be present,

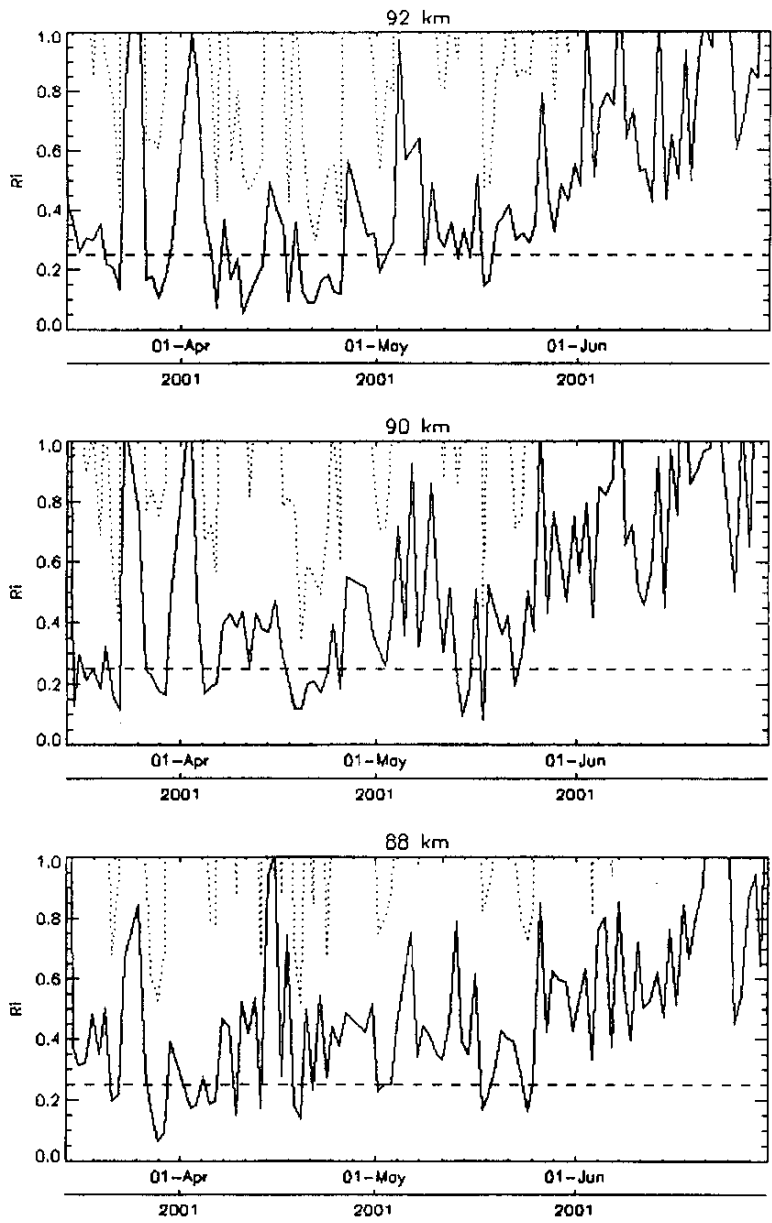


Fig. 6. Richardson Numbers, Ri , derived from the wind field at three selected heights. The dotted lines denote the day-average Ri whereas the solid lines denote these values minus the standard deviation. The standard deviation here reflects the day-variability in wind shear, and not the error. A dashed line denotes the $Ri = 0.25$ condition. That the solid line drops below 0.25 on occasion is an indication of a probability of dynamic instability and therefore neutral air turbulence. Note that there are instances of dynamic instability before the transition to the summer state of the mesosphere, whereas during the summer itself, the mesosphere was dynamically stable.

but we are unable to detect these with the method used here.

4 Summary

We have presented some first results from the newly established meteor radar on Svalbard. Here we have concentrated on small scale features of the atmosphere and their behaviour over the transition from spring to summer states in the polar mesosphere ; first results of larger scale dynamics have been presented in a parallel publication by Aso *et al.* (2001). Even though the dataset is as yet of limited extent , we have already identified two features of the polar mesosphere region :

(i) The summer mesopause appeared (at least in 2001) at around 95 km at 80°N as opposed to a scale height lower down as might have been expected (Hedin 1991) , in particular in view of our experience from observations at 70°N.

(ii) Prior to the transition to a summer state , the upper mesosphere appears prone to dynamic instability and therefore neutral air turbulence , whereas the summer state is characterised by more stable conditions.

The meteor radar , NSMR , is in continuous operation and it is hoped that it will remain so such that eventually interannual and climatic changes may be investigated in temperatures and scales of dynamics from turbulence to mean winds.

Acknowledgments The authors are indebted to the following persons for assistance with construction and maintenance of NSMR : Knut Sandaker , Jürgen R⁹ ttger , J⁹ rg Trautner , Chris Adami .

References

- Dyrud LP , Oppenheim MM , Endt vom AF (2001) : The anomalous diffusion of meteor trails. *Geophys. Res. Lett.* , 28 : 2775 - 2778.
- Hall CM , Aso T (1999) : Mesospheric velocities and buoyancy subrange spectral slopes determined over Svalbard by ESR. *Geophys. Res. Lett.* , 26 : 1685 - 1688.
- Hedin AE (1991) : Extension of the MSIS thermosphere model into the middle and lower atmosphere. *J. Geophys. Res.* , 96 : 1159 - 1172.
- Hocking WK , Thayaparan T (1997) : Simultaneous and colocated observation of winds and tides by MF and meteor radars over London , Canada (43°N , 81°W) , during 1994 - 1996. *Radio Sci.* , 32 : 833 - 865.
- Hocking WK , Thayaparan T , Jones J (1997) : Meteor decay times and their use in determining a diagnostic mesospheric temperature-pressure parameter : methodology and one year of data. *Geophys. Res. Lett.* , 24 : 2977 - 2980.
- Hocking WK (1999) : Temperatures using radar-meteor decay times. *Geophys. Res. Lett.* , 26 : 3297 - 3300.
- Jones W (1995) : The decay of radar echoes from meteors with particular reference to their use in the determination of temperature-fluctuations near the mesopause. *Ann. Geophys.* , 13 : 1104 - 1106.
- Jones J , Webster AR , Hocking WK (1998) : An improved interferometer design for use with meteor radars. *Radio Sci.* , 33 : 55 - 56.
- Roper RG , Brosnahan JW (1997) : Imaging Doppler interferometry and the measurement of atmospheric turbulence. *Radio Sci.* , 32 : 1137 - 1148.
- R⁹ ttger J (2000) : Radar investigation of the mesosphere , stratosphere and the troposphere in Svalbard. *Adv. Polar Upper Atmos. Res.* , 14 : 202 - 220.
- Tsutsumi M , Tsuda T , Nakamura T , Fukao S (1994) : Temperature fluctuations near the mesopause inferred from meteor observations with the middle and upper atmosphere radar. *Radio Sci.* , 29 : 599 - 610.
- Tsutsumi M , Holdsworth D , Nakamura T , Reid J (1999) : Meteor observations with an MF radar. *Earth , Planets Space* ,

51 : 691 – 699.

Wannberg UG , Wolf I , Vanhainen LG , Koskenniemi K , R⁹ ttger J , Postila M , Markannen J , Jacobsen R , Stenberg A , Larsen R , Eliassen S , Heck S , Huskonnen A (1997) : The EISCAT Svalbard Radar , a case study in modern incoherent scatter radar system design. *Radio Sci.* , 32 : 2283 – 2307 .